MEKOMETER MEASUREMENTS IN THE IMPERIAL VALLEY

R.G. Mason, C.N. Crook
and P.R. Wood

Geology Department
Imperial College
London SW7 2BP, England

USGS CONTRACT NO. 14-08-0001-92067
Supported by the EARTHQUAKE HAZARDS REDUCTION PROGRAM

OPEN-FILE NO.80-2008

U.S. Geological Survey
OPEN FILE REPORT
This report was prepared under contract to the U.S. Geological Survey and has not been reviewed for conformity with USGS editorial standards and stratigraphic nomenclature. Opinions and conclusions expressed herein do not necessarily represent those of the USGS. Any use of trade names is for descriptive purposes only and does not imply endorsement by the USGS.

MEKOMETER MEASUREMENTS IN THE IMPERIAL VALLEY

Purchase order no. 92067

R.G. Mason, C.N. Crook and P.R. Wood
Geology Department
Imperial College
London SW7 2BP, England
(011-441) 589-5111

1. Introduction

During the six weeks following the October 15, 1979 earthquake, parts of the Imperial Valley Mekometer network (Fig. 1) around the Imperial fault to the east of El Centro were re-measured, some repeatedly, in an attempt to assess the coseismic and postearthquake slip on the fault, and horizontal strain adjustment around it. This report presents the results, together with the most recent pre-earthquake measurements, for comparison. It includes also a brief discussion of the results.

2. The measurements

Measurements were started on October 21, 1979, six days after the earthquake, and continued through November 28, during which period a total of 405 length measurements were made, involving 184 lines. The instrument used was Kern Mekometer Ser. No. 218020, with which the 1978 and Spring, 1979 measurements had been made. The results, corrected for instrumental and atmospheric factors, are presented in Table 1, together with the most recent pre-earthquake measurements. Relative positions of the lines are indicated schematically in Fig. 2. From repeat measurements, and other factors, the standard error of a corrected length is estimated to be about 1.5 mm.

Six days after the earthquake, the fault was creeping at a rate of between 5 mm and 10 mm/day. The first objective was therefore to monitor the changing deformation, both on and away from the fault. This was achieved by repeated measurements of the small Heber Road and Tuttle Ranch networks, and of the star-like patterns of lines radiating from seven selected stations (Fig. 3), each of which could be measured within a span of about two hours. Stars centered on three of the stations, H33, M2955 and R27, together with the two small networks, served to monitor deformation on the fault. Deformation away from the fault was monitored by four stars, centered on stations Q32 and W31, about 3 km and 10 km respectively, from the fault on its southwest side, and stations E30 and D21 at similar distances on its northeast side. The fault-crossing figures were measured four or five times during the six weeks, the close-in stars three times, and the more distant ones twice.

The stars and the Heber Road and Tuttle Ranch networks provide information at widely separated points. In order to obtain a more detailed picture of the variation of deformation both along and across the fault, three chains of triangles, each between 9 km and 10 km long, were measured once only, a "north chain" and a "south chain" approximately normal to the fault, to provide profiles of deformation across it, and a "fault chain" to measure the variation of deformation along it. The first two were measured during the third week after the earthquake, and the last during the seventh week, by which time the fault was creeping at a rate of less than 1 mm/day.

3. Postearthquake fault slip

In analyzing results from the fault-crossing figures, it has been assumed that all length changes are due to slip, no account being taken of strain. The displacements, as calculated relative to the April, 1979 survey data, are shown in Fig. 4. Afterslip is in the same sense as displacement associated with the main event, and over a period of six weeks it will have contributed as much as 25% to the total fault slip.

The observations can be well fitted with an exponential decay model:

$$\delta = a + be^{-ct}$$

where δ = displacement and t = days after the event. a is the predicted total fault slip at the particular location, and b the predicted postseismic slip. The time constant c was found to have almost the same value at all four locations, and a common value of 0.06 was adopted for the final fit. It follows that half the predicted postseismic slip will have occurred within about twelve days of the earthquake, and at least 94% within six weeks.

It should be noted that the above results include any slip that may have occurred between the April 1979 survey and the time of the earthquake. If deformation had continued at the average rate observed between 1975 and the Spring of 1979, the fault could not have slipped by more than 5 mm during this period, but in view of the known episodic nature of the fault creep (Goulty et al., 1978), with creep events sometimes exceeding 10 mm, very much larger changes might have occurred.

Although the Tuttle Ranch quadrilateral spans the 1940 trace of the Imperial fault, the 1979 break did not extend this far south. Changes of up to 160 microstrain were observed between preearthquake and postearthquake measurements, mainly of E-W extension, but the pattern is neither uniform nor consistent with simple fault slip. It is most satisfactorily described by the NW station having moved about 10 cm to the west, the other three stations remaining fixed, but there is no evidence on the ground to support such a movement.

4. Variation of slip along the fault

In computing displacement vectors for stations of the fault chain, it has been assumed that the position of station H32, near the fault at one end of the chain, and the direction of the line joining it and station P28, on the same side of the fault at the opposite end, have not changed as a result of the earthquake. The results, plotted in Fig. 5 after being "balanced" about the fault by the addition of a common vector, represent relative movement between April 1979 and the seventh week after the earthquake.

In order to arrive at approximate values for slip on the fault, the computed displacements have been modelled with a linear variation of slip with distance along the fault, together with uniform shears parallel to it on either side. The results indicate right-lateral shears on both sides of the fault, with values of about 300 $\pm$ 100 microstrain on the southwest side and 60 $\pm$ 64 microstrain on the northeast (errors represent one s.e.). Fig. 6 shows the displacements of the two edges of the fault, relative to station H32 held fixed, corrected for shear, also their difference, representing slip on the fault. The latter varies from about 45 cm at the northwest end of the chain to about 60 cm at the southeast, in reasonable agreement with values derived independently from the fault-crossing figures. At Heber Road, 3 km beyond the southeastern end of the chain, the displacement seven weeks after the earthquake amounted to about 70 cm, confirming the general increase in dispalcement from north to south.

5. Variation of strain away from the fault

Of the various figures giving information about deformation away from the fault, the north and south chains were surveyed once only, during the third week after the earthquake, and provide profiles of mainly coseismic strain normal to the fault, while the four stars D21, E30, Q33 and W41 were measured several times, and provide a measure of strain adjustment.

Principal strains calculated for figures of the north and south chains are shown in Fig. 7, while Fig. 8 presents the same information in the form of profiles of the strain components e_{11}, e_{22} and γ_2 ($= e_{12} + e_{21}$), calculated for axes orthogonal to the fault strike. At first sight, the lines would appear to have little in common. However, the two lines extend to different distances on each side of the fault, and if those parts common to both are compared, i.e. up to $2\frac{1}{2}$ km on the southwest side and 3 km on the northeast, points of similarity emerge: (1) relatively small values of linear strain parallel to the fault (e_{11}), except in the vicinity of the Brawley fault on the north line, where it increases to more than 300 microstrain, (2) the component of linear strain normal to the fault (e_{22}) is extensional on the southwest side of the fault and compressional on the northeast, and (3) γ_2 is positive on the southwest side of the fault, with markedly high values close to it, which indicates right-lateral shear parallel to the fault.

As might have been expected, the stars more distant from the fault show very much smaller changes between preearthquake and postearthquake surveys than those nearer to it. Thus at D21, 9 km northeast of the fault, and W41, 11 km southwest of it, the dominant strain changes were left-lateral shears parallel to the fault, of less than 25 and 10 microstrain, respectively. During the several weeks of observation, changes on figures not crossing the fault were small, generally not exceeding 3 microstrain.

6. Conclusions

This small sample of the information derivable from the Mekometer network has revealed a complex pattern of coseismic strain changes. Some of this complexity almost certainly reflects the influence of unmapped faults, or even bifurcations of the Imperial fault itself. In particular, movement on the Brawley fault, whose mapped surface trace terminates just to the north of the network, has clearly affected strains on the north line.

One consequence that might have been expected of right-lateral slip on the fault is a relaxation of shear strain in a left-lateral sense on either side. This would be indicated by negative values of γ_2 in Fig. 8, or by axes of maximum right-lateral shear strain normal to the fault (see Fig. 9). This is in fact the case on the northeast side of the fault, except in the vicinity of the Brawley fault, but on the southwest side the change has been in the opposite sense, with the development on both lines of right-lateral shear parallel to the fault. This might be interpreted in terms of right-lateral slip sub-parallel to the Imperial fault.

A result that had not been expected is the large relative displacements, both parallel and normal to the fault, between points several km apart. This is illustrated in Fig. 10, which shows relative displacements parallel to the fault derived directly from the fault chain measurements, and displacements normal to it derived from the computed values of e_{22} along the north and south chains. Thus points about $2\frac{1}{2}$ km from the fault on its southwest side have moved away from it by up to 25 cm, while points at a similar distance from the fault on its northeast side have moved towards it by as much as 50 cm. These movements imply a complicated pattern of radiated energy.

Reference

Goulty, N.R., Burford, R.O., Allen, C.R., Gilman, R., Johnson, C.E. and Keller, R.P., 1978. Large creep events on the Imperial Fault, California. Seismol. Soc. America, 68, 517-521.

TABLE 1: IMPERIAL VALLEY LINE LENGTHS, OCTOBER/NOVEMBER 1979, AND MOST RECENT PRE-EARTHQUAKE LENGTHS (IN METERS).

LINE	DATE	LENGTH	DATE	LENGTH
D20-D21	28OCT79	798.8217	7FEB75	.8339
	21NOV79	.8246		
D21-D22	28OCT79	817.8767	25FEB75	.8875
	21NOV79	.8776		
D21-E20	28OCT79	1135.4769	7FEB75	.5016
	21NOV79	.4811		
D21-E21	28OCT79	801.5790	7FEB75	.5867
	21NOV79	.5823		
D21-E22	28OCT79	1146.3459	24FEB75	.3523
	21NOV79	.3486		
D28-D29	3NOV79	753.2308	11DEC78	.3483
D28-E28	3NOV79	837.1662	11DEC78	.0704
D28-E29	3NOV79	1113.2458	11DEC78	.2539
D29-D30	3NOV79	804.9416		
D29-E29	3NOV79	792.4749	8AUG78	.4114
D29-E30	24OCT79	1122.4266	10MAY79	.4670
	2NOV79	.4280		
	24NOV79	.4266		
D30-D31	3NOV79	802.9057	5MAY79	.9786
D30-E29	3NOV79	1141.9931	5MAY79	2.0013
D30-E30	23OCT79	828.1204	5MAY79	.0177
	24OCT79	.1206		
	2NOV79	.1230		
	24NOV79	.1226		
D30-E31	3NOV79	1148.5205	5MAY79	.5944
D31-E30	24OCT79	1112.6108	8MAY79	.5796
	2NOV79	.6127		
	24NOV79	.6117		
D31-E31	3NOV79	754.9221	5MAY79	.8974
E28-E29	3NOV79	610.1482	11DEC78	.2660
E29-E30	24OCT79	777.3418	10MAY79	.4784
	2NOV79	.3397		
	3NOV79	.3403		
	24NOV79	.3421		
E29-F29	3NOV79	791.0183	10AUG78	.0030
E29-F30	3NOV79	1110.3777	9AUG78	.4990
E30-E31	24OCT79	813.7481	8MAY79	.8544
	2NOV79	.7492		
	24NOV79	.7483		
E30-F29	24OCT79	1117.9399	10MAY79	8.0197
	2NOV79	.9360		
	24NOV79	.9352		
E30-F30	23OCT79	789.7713	10MAY79	.7377
	24OCT79	.7730		
	2NOV79	.7731		
	24NOV79	.7734		
E30-F31	24OCT79	1136.6951	10MAY79	.8108
	2NOV79	.6992		
	24NOV79	.6996		

TABLE 1: IMPERIAL VALLEY LINE LENGTHS, OCTOBER/NOVEMBER 1979, AND MOST RECENT PRE-EARTHQUAKE LENGTHS (IN METERS).

LINE	DATE	LENGTH	DATE	LENGTH
E31-F31	3NOV79	794.2423	5MAY79	.1279
E31-F32	3NOV79	1068.2453	7MAY79	.3222
F30-H30	23OCT79	1403.5477	10JLY78	.6873
F31-F32	4NOV79	724.1389	8MAY79	.0657
F31-G32	4NOV79	1360.5602	10MAY79	.8212
F32-F33	4NOV79	1031.3080	8MAY79	.3648
F32-G32	4NOV79	1188.6720	9MAY79	.7250
F32-G33	4NOV79	1303.8203	8MAY79	4.0500
F33-G33	4NOV79	810.8747	8MAY79	.8883
F33-G34	4NOV79	1168.3934	8MAY79	.5477
G32-G33	4NOV79	1142.7681	9MAY79	.7254
G32-H33	20NOV79	1182.0129	10MAY79	.0657
G33-G34	4NOV79	796.1232	8MAY79	5.8875
G33-H33	25OCT79	932.5213	9MAY79	.8899
	28OCT79	.5154		
	4NOV79	.5021		
	12NOV79	.4891		
	20NOV79	.4824		
G34-H33	25OCT79	1206.7717	10MAY79	.7542
	28OCT79	.7729		
	4NOV79	.7752		
	12NOV79	.7746		
	20NOV79	.7771		
G34-H34	4NOV79	764.5856	2JLY78	.7144
H30-J30	23OCT79	1006.1772	25JUN78	.4245
H32-H33	25OCT79	948.3571	10MAY79	.1873
	28OCT79	.3666		
	4NOV79	.3761		
	12NOV79	.3834		
	20NOV79	.3907		
H32-J31	26NOV79	1092.3111	25JUN78	.3413
H32-J32	25NOV79	814.2821	5AUG78	.7223
H33-H34	25OCT79	817.1182	2JLY78	6.9543
	28OCT79	.1180		
	4NOV79	.1184		
	12NOV79	.1186		
	20NOV79	.1199		
H33-J32	25OCT79	1089.1476	10MAY79	.0262
	28OCT79	.1514		
	4NOV79	.1500		
	12NOV79	.1500		
	20NOV79	.1511		
H33-J33	25OCT79	678.6255	10MAY79	.7662
	28OCT79	.6243		
	4NOV79	.6230		
	12NOV79	.6217		
	20NOV79	.6217		

TABLE 1: IMPERIAL VALLEY LINE LENGTHS, OCTOBER/NOVEMBER 1979, AND MOST RECENT PRE-EARTHQUAKE LENGTHS (IN METERS).

LINE	DATE	LENGTH	DATE	LENGTH
H33-J34	28OCT79	1055.4865	10MAY79	.4528
	4NOV79	.4852		
	12NOV79	.4842		
	20NOV79	.4844		
H34-J34	4NOV79	801.3719	23JUN78	.4076
J30-K30	23OCT79	791.4889	9JUN78	.5656
J31-J32	25NOV79	892.1103	14JUN78	1.9780
	26NOV79	.1173		
J31-K31	26NOV79	840.7119	8JUN78	.8078
J31-K32	26NOV79	1160.5469	15JUN78	.7963
J32-K31	26NOV79	1178.6925	6JUN78	.3220
J32-K32	26NOV79	799.8666	17JUN78	.9954
J33-J34	4NOV79	779.3359	19JUN78	.1938
J33-K34	5NOV79	1120.2854	20JUN78	.1978
J34-K34	4NOV79	802.1785	20JUN78	.2167
J34-K35	4NOV79	1148.6779	21JUN78	.5104
K26-K27	1NOV79	740.8840	6AUG78	1.1791
K26-L27	1NOV79	1212.5318	5DEC78	.7493
K27-L26	1NOV79	1165.8485	12DEC78	.8940
K27-L27	1NOV79	866.4918	5DEC78	.4714
K27-L28	1NOV79	1408.2219	4DEC78	.4117
K30-L30	23OCT79	889.4557	8JUN78	.5028
K31-K32	26NOV79	779.8525	12JUN78	.5943
K31-L30	26NOV79	1139.0811	11JUN78	.1432
K31-L31	26NOV79	908.5817	6JUN78	9.0800
K32-L31	26NOV79	1182.4761	12JUN78	.5115
K34-K35	5NOV79	827.7440	22JUN78	.5854
K34-L35	5NOV79	1328.3048	19AUG78	.1154
K35-L35	5NOV79	1056.8614	19AUG78	.8916
L26-L27	1NOV79	822.6456	9DEC78	.6914
L27-L28	1NOV79	842.5462	5DEC78	.7521
L27-M28	1NOV79	1210.0683	5DEC78	.3213
L28-L29	31OCT79	786.5855	4DEC78	.7469
L28-M28	1NOV79	627.4180	4DEC78	.4471
L29-L30	27NOV79	968.3250	12JUN78	.3215
L29-M28	31OCT79	992.9381	4DEC78	.9841
L29-M29	31OCT79	622.3629	15JUN78	.3786
L29-M30	31OCT79	1042.4782	15JUN78	.6232
	27NOV79	.4813		
L29-N29	27NOV79	1385.0253		
L29A-L30	27NOV79	942.1102		
L29A-M30	27NOV79	1028.5526		
L29A-N29	27NOV79	1394.6505		
L30-L31	27NOV79	719.3421	7JUN78	.1719
L30-M29	27NOV79	1268.1771	11JUN78	.1260
L30-M30	23OCT79	854.6109	13JUN78	5.1000
	7NOV79	.5659		
	27NOV79	.5471		

TABLE 1: IMPERIAL VALLEY LINE LENGTHS, OCTOBER/NOVEMBER 1979, AND MOST RECENT PRE-EARTHQUAKE LENGTHS (IN METERS).

LINE	DATE	LENGTH	DATE	LENGTH
L31-M30	27NOV79	1163.2498	15JUN78	.3014
M28-M29	1NOV79	785.3576	4DEC78	.5394
M29-M2955	22OCT79	600.8921	25APR79	1.0431
	26OCT79	.8905		
	1NOV79	.8884		
	11NOV79	.8832		
	19NOV79	.8843		
M29-M30	31OCT79	837.5624	15JUN78	.2939
	7NOV79	.5730		
	27NOV79	.5917		
M29-N29	7NOV79	762.6674	21APR79	.6904
	27NOV79	.6717		
M29-N30	31OCT79	1091.6974	2DEC78	.9168
M2905-M2955	22OCT79	426.1885	26APR79	.6268
	26OCT79	.1689		
	1NOV79	.1522		
	11NOV79	.1350		
	19NOV79	.1247		
M2950-M2955	21OCT79	414.3565	26APR79	.1862
	22OCT79	.3583		
	26OCT79	.3702		
	1NOV79	.3788		
	11NOV79	.3890		
	19NOV79	.3966		
M2950-N29	21OCT79	409.3742	26APR79	.3834
M2950-N2905	21OCT79	592.9929	27APR79	3.1754
M2955-M30	22OCT79	580.5474	25APR79	.5416
	26OCT79	.5483		
	1NOV79	.5476		
	11NOV79	.5465		
	19NOV79	.5504		
M2955-M3050	22OCT79	377.0564	26APR79	.0237
	26OCT79	.0566		
	1NOV79	.0581		
	11NOV79	.0574		
	19NOV79	.0579		
M2955-N29	21OCT79	551.3912	25APR79	0.9148
	22OCT79	.3954		
	26OCT79	.4194		
	1NOV79	.4421		
	11NOV79	.4613		
	19NOV79	.4757		
	27NOV79	.4807		

TABLE 1: IMPERIAL VALLEY LINE LENGTHS, OCTOBER/NOVEMBER 1979, AND MOST RECENT PRE-EARTHQUAKE LENGTHS (IN METERS).

LINE	DATE	LENGTH	DATE	LENGTH
M2955-N2905	21OCT79	369.2751	26APR79	.3213
	22OCT79	.2724		
	26OCT79	.2734		
	1NOV79	.2747		
	11NOV79	.2734		
	19NOV79	.2769		
M2955-N30	22OCT79	490.8103	25APR79	.8766
	26OCT79	.8102		
	1NOV79	.8117		
	11NOV79	.8101		
	19NOV79	.8125		
M30-N29	23OCT79	1129.8706	21APR79	.3596
	7NOV79	.9177		
	27NOV79	.9501		
M30-N30	31OCT79	758.1472	22APR79	.2624
	7NOV79	.1493		
	27NOV79	.1517		
M30-N31	31OCT79	1100.9182		
N28-N29	27NOV79	779.4592	21APR79	.5184
N28-P28	28NOV79	867.8043	20APR79	.8157
N28-P29	27NOV79	1153.3885	20APR79	.6992
N29-N2905	21OCT79	426.4558	26APR79	.2083
N29-N30	7NOV79	783.2796	22APR79	2.9580
	27NOV79	.2998		
N29-P29	23OCT79	811.4853	21APR79	2.0268
	27NOV79	.4273		
N30-N31	31OCT79	849.7398	22APR79	.6699
N30-P29	27NOV79	1123.5955	21APR79	.5627
N30-P31	31OCT79	1181.9299	22APR79	.8172
N31-N32	31OCT79	761.6700	11JUN78	.5672
N31-P31	31OCT79	820.8194	1DEC78	.7827
N31-P32	31OCT79	1142.9608	1DEC78	.8093
N32-P31	31OCT79	1115.3183	1DEC78	.2879
N32-P33	31OCT79	1250.5665	10NOV78	.4398
P28-P29	27NOV79	925.1257	19APR79	4.7502
P28-Q27	28NOV79	976.0454	15APR79	.1035
P28-Q28	28NOV79	777.1037	15APR79	.6492
P29-Q28	27NOV79	1130.4236	20APR79	.3878
P29-Q29	23OCT79	749.8928	20APR79	.9090
P31-P32	31OCT79	772.2418	1DEC78	.1480
P31-Q32A	31OCT79	1115.2512		
P32-P33	31OCT79	906.5955	21NOV78	.5016
P32-Q32A	31OCT79	803.5366		
P32-Q33	24OCT79	1189.9955	20NOV78	.8468
	30OCT79	.9963		
	10NOV79	.9957		
	23NOV79	.9965		

TABLE 1: IMPERIAL VALLEY LINE LENGTHS, OCTOBER/NOVEMBER 1979, AND MOST RECENT PRE-EARTHQUAKE LENGTHS (IN METERS).

LINE	DATE	LENGTH	DATE	LENGTH
P33-Q33	24OCT79	823.9476	10NOV78	.8660
	30OCT79	.9508		
	10NOV79	.9499		
	23NOV79	.9512		
P33-Q34	30OCT79	1123.3133	10NOV78	.2871
P34-Q33	24OCT79	1182.5905	10NOV78	.5411
	10NOV79	.5906		
	23NOV79	.5924		
Q26-R27	27OCT79	1163.3592	9APR79	.5437
	2NOV79	.3653		
	11NOV79	.3637		
	21NOV79	.3648		
Q27-Q28	28NOV79	821.5858	10APR79	.4200
Q27-R27	27OCT79	931.3705	9APR79	.4018
	2NOV79	.3725		
	11NOV79	.3725		
	21NOV79	.3715		
Q28-R27	27OCT79	1181.7071	9APR79	.1431
	2NOV79	.7241		
	11NOV79	.7422		
	21NOV79	.7536		
	28NOV79	.7698		
Q28-R28	28NOV79	833.7428	9APR79	.7685
Q29-R29	23OCT79	869.1067	19APR79	.0743
Q32A-Q33	30OCT79	869.6354		
	10NOV79	.6316		
	23NOV79	.6312		
Q33-Q34	24OCT79	836.8827	9NOV78	.9109
	30OCT79	.8862		
	10NOV79	.8822		
	23NOV79	.8833		
Q33-R32	24OCT79	1145.4644	8NOV78	.4657
	10NOV79	.4627		
	23NOV79	.4609		
Q33-R33	24OCT79	783.7063	8NOV78	.7096
	10NOV79	.7059		
	23NOV79	.7080		
Q33-R34	24OCT79	1075.3316	7NOV78	.4353
	30OCT79	.3354		
	10NOV79	.3293		
	23NOV79	.3325		
Q34-R34	30OCT79	801.1304	7NOV78	.1483
Q34-R35	30OCT79	1118.8344	7NOV78	.9433
R26-R27	27OCT79	814.9172	12APR79	5.0419
	2NOV79	.9202		
	11NOV79	.9156		
	21NOV79	.9176		

TABLE 1: IMPERIAL VALLEY LINE LENGTHS, OCTOBER/NOVEMBER 1979, AND MOST RECENT PRE-EARTHQUAKE LENGTHS (IN METERS).

LINE	DATE	LENGTH	DATE	LENGTH
R27-R28	27OCT79	818.4375	7APR79	.1459
	2NOV79	.4444		
	11NOV79	.4575		
	21NOV79	.4612		
R27-S26	27OCT79	1155.1273	8APR79	.0872
	2NOV79	.1306		
	11NOV79	.1259		
	21NOV79	.1279		
R27-S27	27OCT79	795.0171	8APR79	.5481
	2NOV79	.0064		
	11NOV79	4.9884		
	21NOV79	.9827		
R27-S28	27OCT79	1129.3467	7APR79	.4656
	2NOV79	.3418		
	11NOV79	.3409		
	21NOV79	.3414		
R29-S29	23OCT79	813.0513	6APR79	.0109
R34-R35	30OCT79	918.5186	5NOV78	.5473
R34-S35	30OCT79	1192.7679	2NOV78	.8104
R35-S35	30OCT79	830.3410	1NOV78	.3194
R35-S36	30OCT79	1150.7983	1NOV78	.8173
S35-S36	30OCT79	809.1982	29OCT78	.2148
V2305-V2355	26OCT79	397.2043	29APR79	.1991
	5NOV79	.2055		
	12NOV79	.2072		
	20NOV79	.2068		
V2305-V24	26OCT79	377.8414	29APR79	.8106
	5NOV79	.8408		
	12NOV79	.8430		
	20NOV79	.8405		
V2305-V2450	26OCT79	581.4991	29APR79	.6506
	5NOV79	.4951		
	12NOV79	.4929		
	20NOV79	.4913		
V2355-V24	26OCT79	482.1280	29APR79	.1152
	5NOV79	.1287		
	12NOV79	.1298		
	20NOV79	.1277		
V2355-V2450	26OCT79	299.0067	29APR79	8.7222
	5NOV79	.0166		
	12NOV79	.0198		
	20NOV79	.0232		
V24-V2405	26OCT79	369.8587	28APR79	.4775
	5NOV79	.8717		
	12NOV79	.8771		
	20NOV79	.8820		

TABLE 1: IMPERIAL VALLEY LINE LENGTHS, OCTOBER/NOVEMBER 1979, AND MOST RECENT PRE-EARTHQUAKE LENGTHS (IN METERS).

LINE	DATE	LENGTH	DATE	LENGTH
V24-V2450	26OCT79	435.7784	28APR79	6.3178
	5NOV79	.7580		
	12NOV79	.7532		
	20NOV79	.7469		
V24-V2455	26OCT79	579.3677	28APR79	.4978
	5NOV79	.3644		
	12NOV79	.3645		
	20NOV79	.3617		
V2405-V2450	26OCT79	564.9837	28APR79	.9677
	5NOV79	.9854		
	12NOV79	.9850		
	20NOV79	.9839		
V2405-V2455	26OCT79	416.0263	27APR79	.0459
	5NOV79	.0289		
	12NOV79	.0272		
	20NOV79	.0262		
V2450-V2455	26OCT79	395.1656	28APR79	.1223
	5NOV79	.1674		
	12NOV79	.1656		
	20NOV79	.1657		
V40-W41	25OCT79	1103.7476	25OCT78	.7511
	23NOV79	.7458		
V41-W41	25OCT79	811.5956	24OCT78	.5939
	23NOV79	.5966		
V42-W41	25OCT79	1172.9352	19OCT78	.9342
	23NOV79	.9363		
W40-W41	25OCT79	788.5635	21OCT78	.5629
	23NOV79	.5632		
W41-W42	25OCT79	854.4499	25OCT78	.4515
	23NOV79	.4512		
W41-X40	25OCT79	1123.3087	21OCT78	.3054
	23NOV79	.3060		
W41-X41	25OCT79	777.7864	25OCT78	.7789
	23NOV79	.7854		
W41-X42	25OCT79	1145.2449	18OCT78	.2353
	23NOV79	.2457		
120-121	22OCT79	685.3187	3MAY79	.2103
	27OCT79	.3165		
	10NOV79	.3214		
	19NOV79	.3218		
120-220	21OCT79	601.9107	3MAY79	.9599
	27OCT79	.9082		
	10NOV79	.9121		
	19NOV79	.9107		
120-221	22OCT79	943.7615	3MAY79	.7944
	27OCT79	.7581		
	10NOV79	.7611		
	19NOV79	.7602		

TABLE 1: IMPERIAL VALLEY LINE LENGTHS, OCTOBER/NOVEMBER 1979, AND MOST RECENT PRE-EARTHQUAKE LENGTHS (IN METERS).

LINE	DATE	LENGTH	DATE	LENGTH
121-220	21OCT79	962.9758	3MAY79	.9168
	27OCT79	.9740		
	10NOV79	.9785		
	19NOV79	.9792		
121-221	22OCT79	656.7125	3MAY79	.7345
	27OCT79	.7093		
	10NOV79	.7097		
	19NOV79	.7094		
220-221	22OCT79	749.7313	3MAY79	.7416
	27OCT79	.7289		
	10NOV79	.7310		
	19NOV79	.7310		

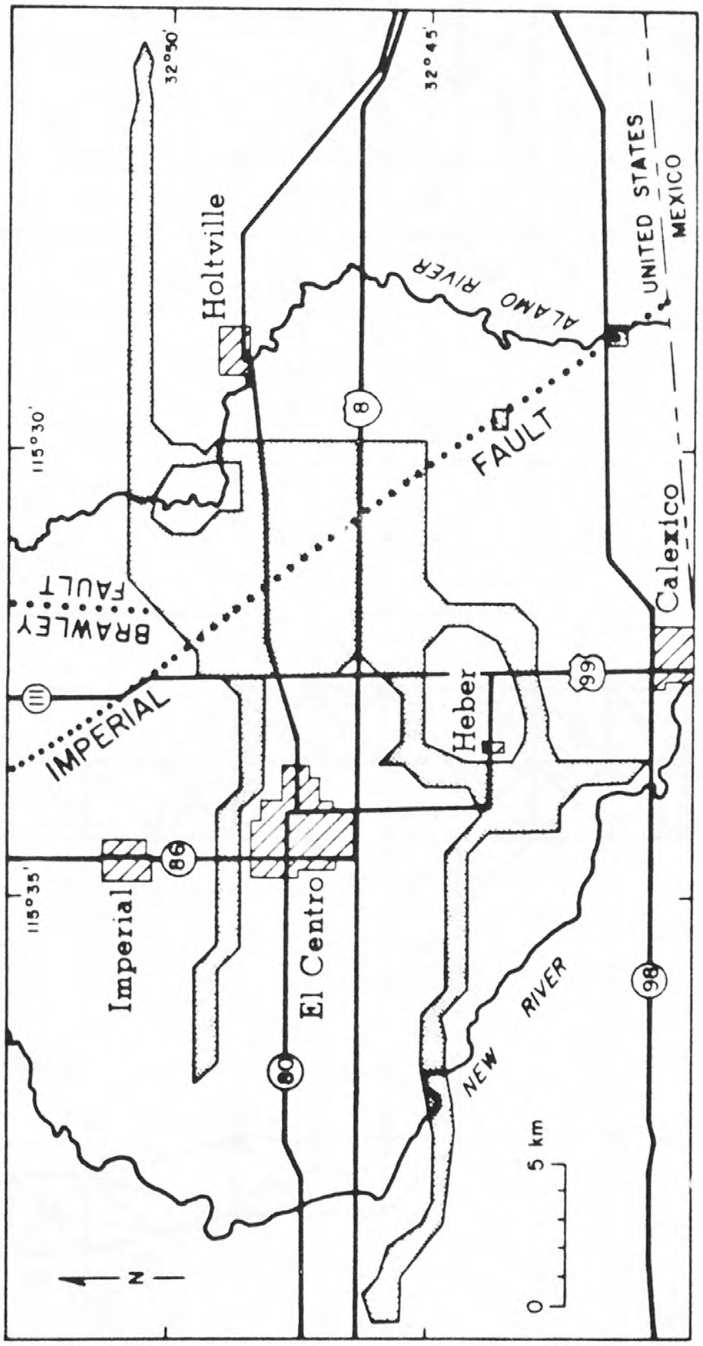

Figure 1. The Imperial Valley Mekometer network.

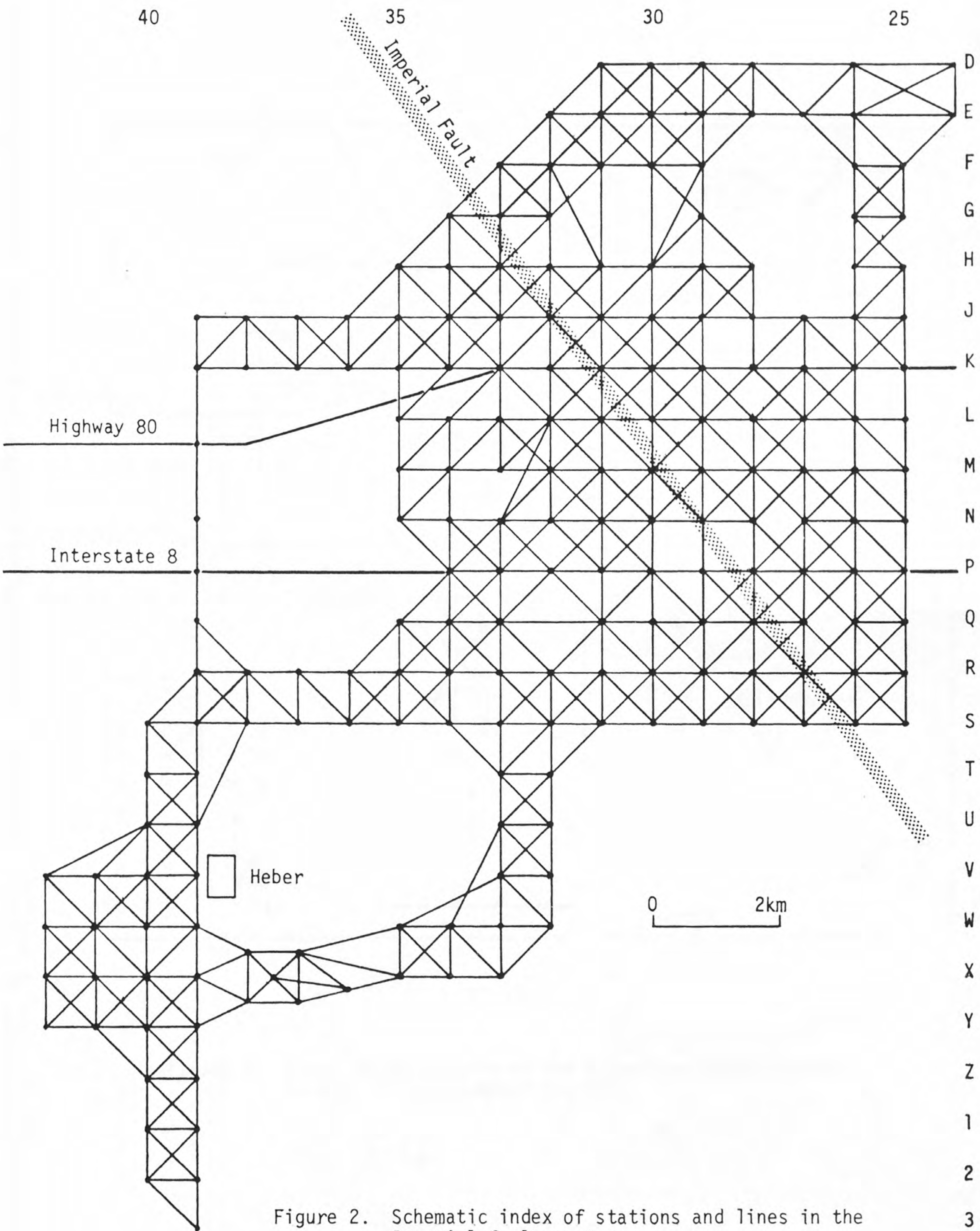

Figure 2. Schematic index of stations and lines in the Imperial fault sector.

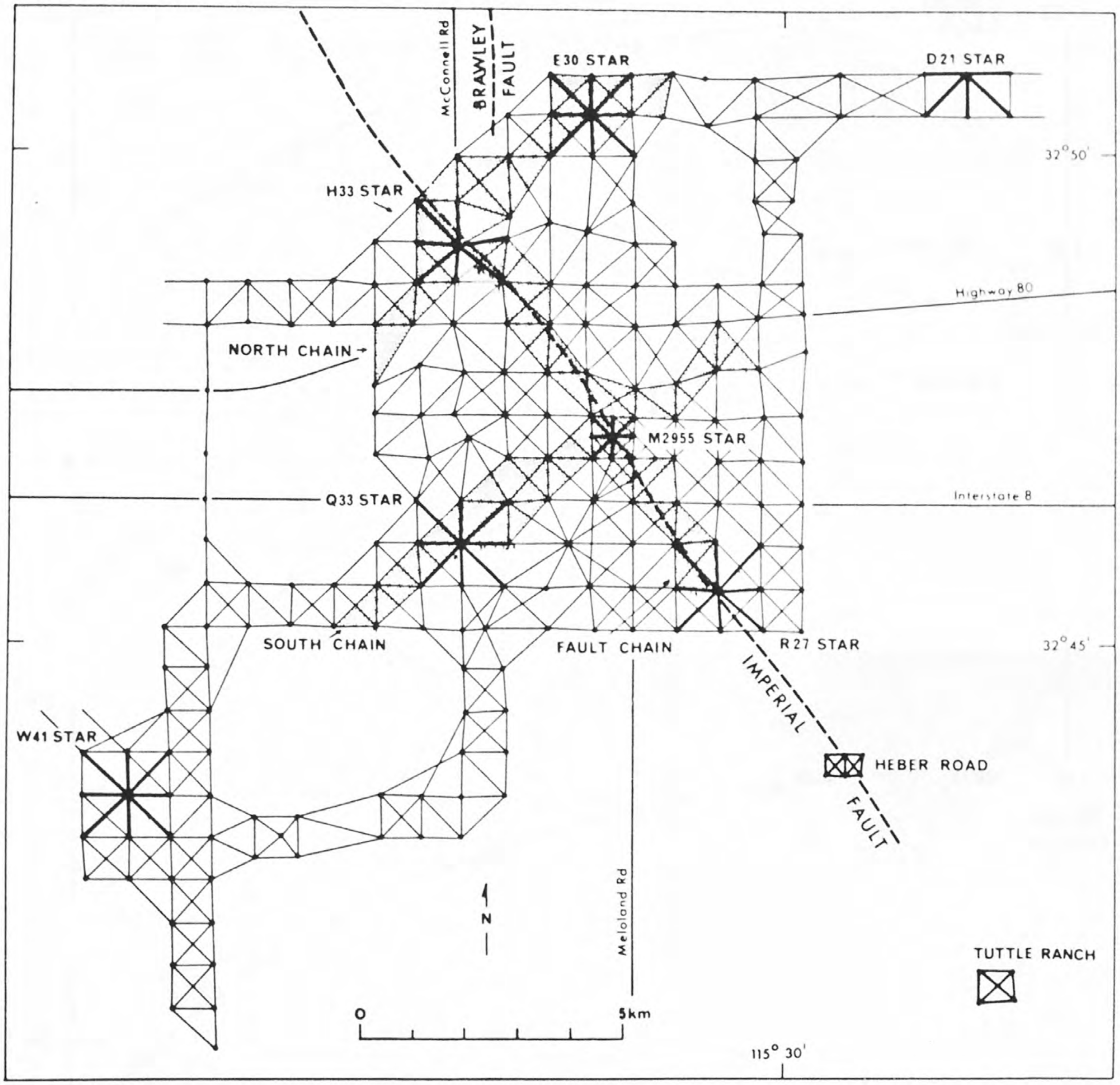

Figure 3. Index to those parts of the network measured between October 21 and November 27, 1979.

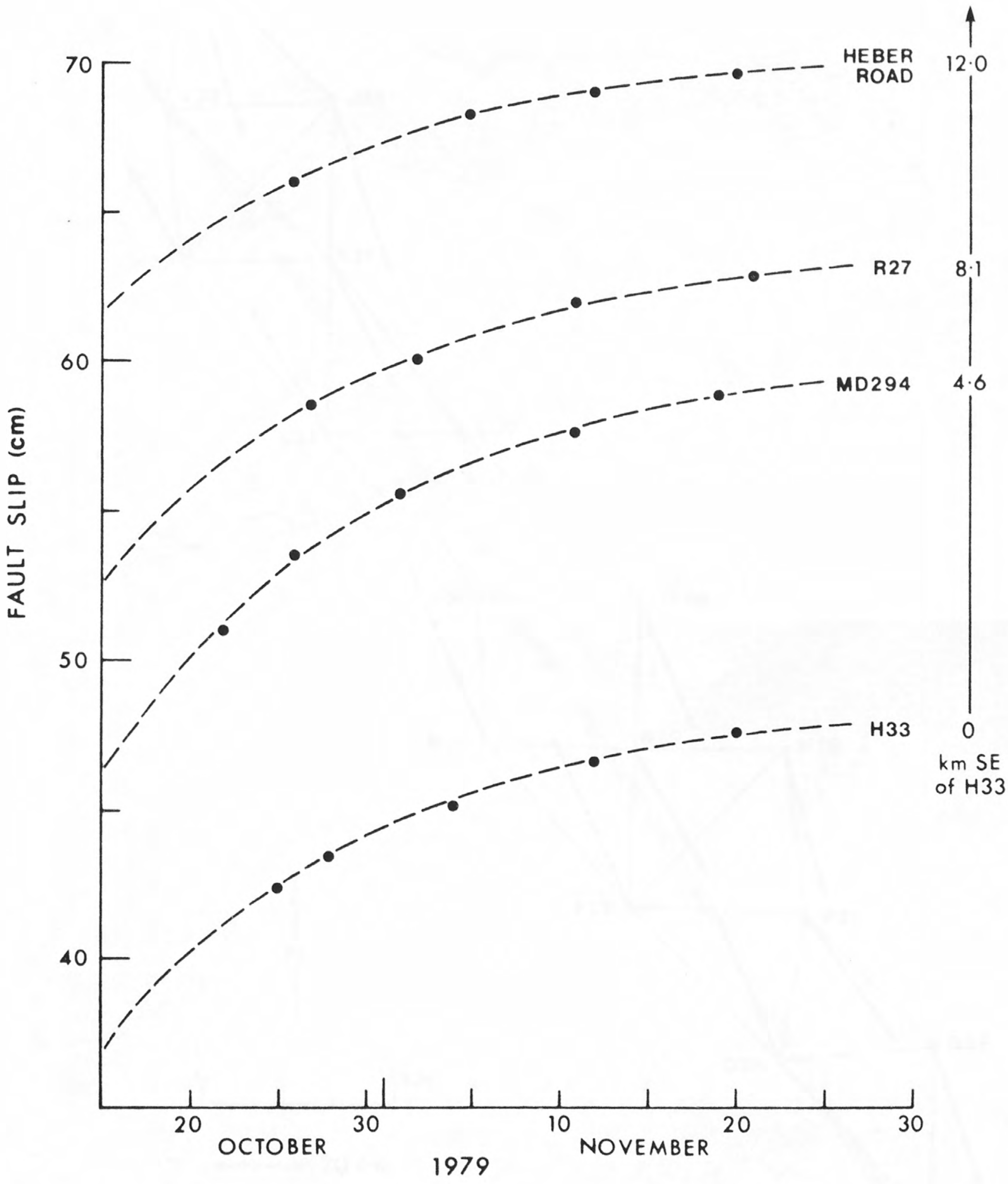

Figure 4. Slip on the Imperial fault since April 1979. The curves are for an exponentially decreasing rate of slip with time.

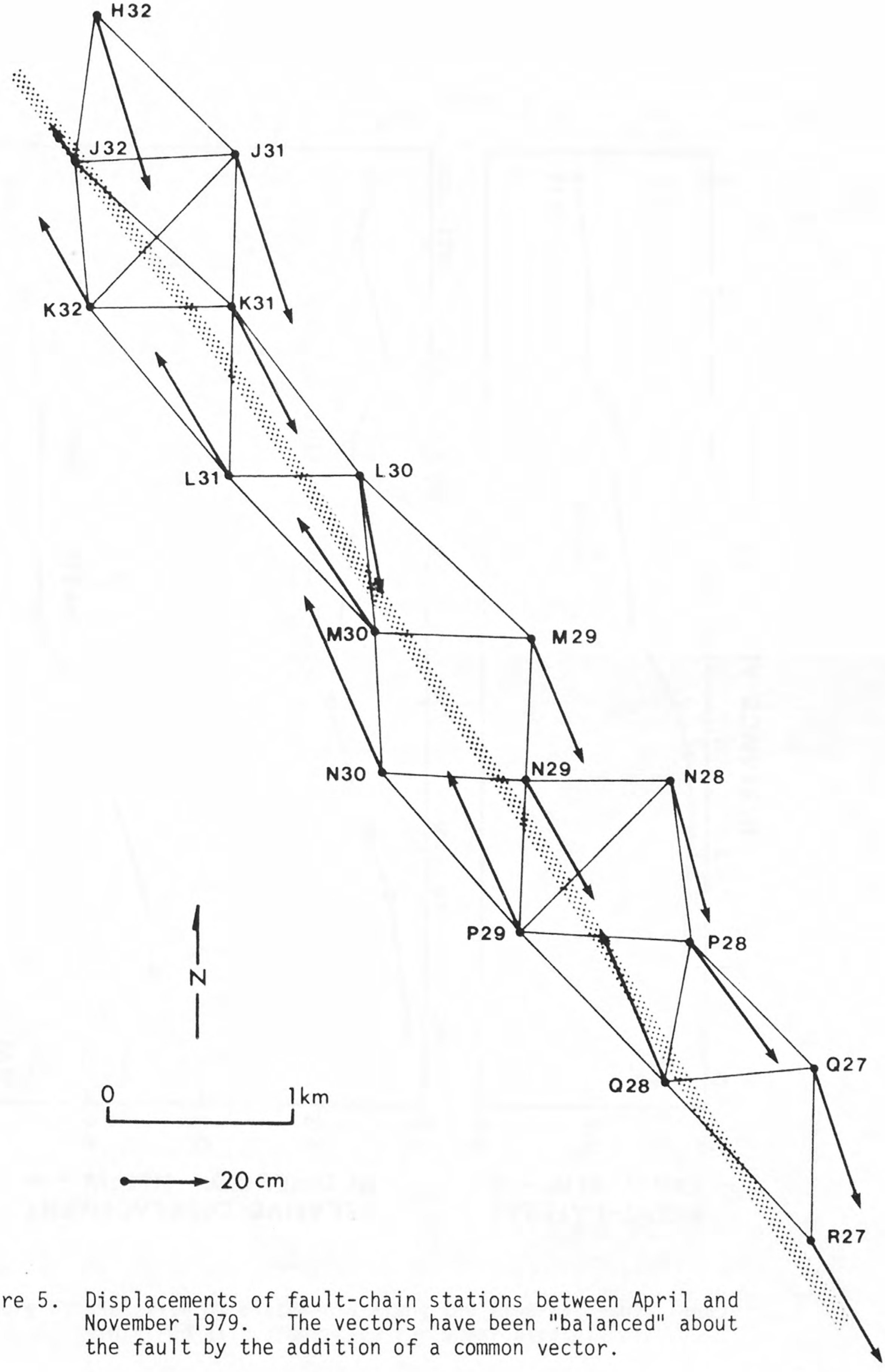

Figure 5. Displacements of fault-chain stations between April and November 1979. The vectors have been "balanced" about the fault by the addition of a common vector.

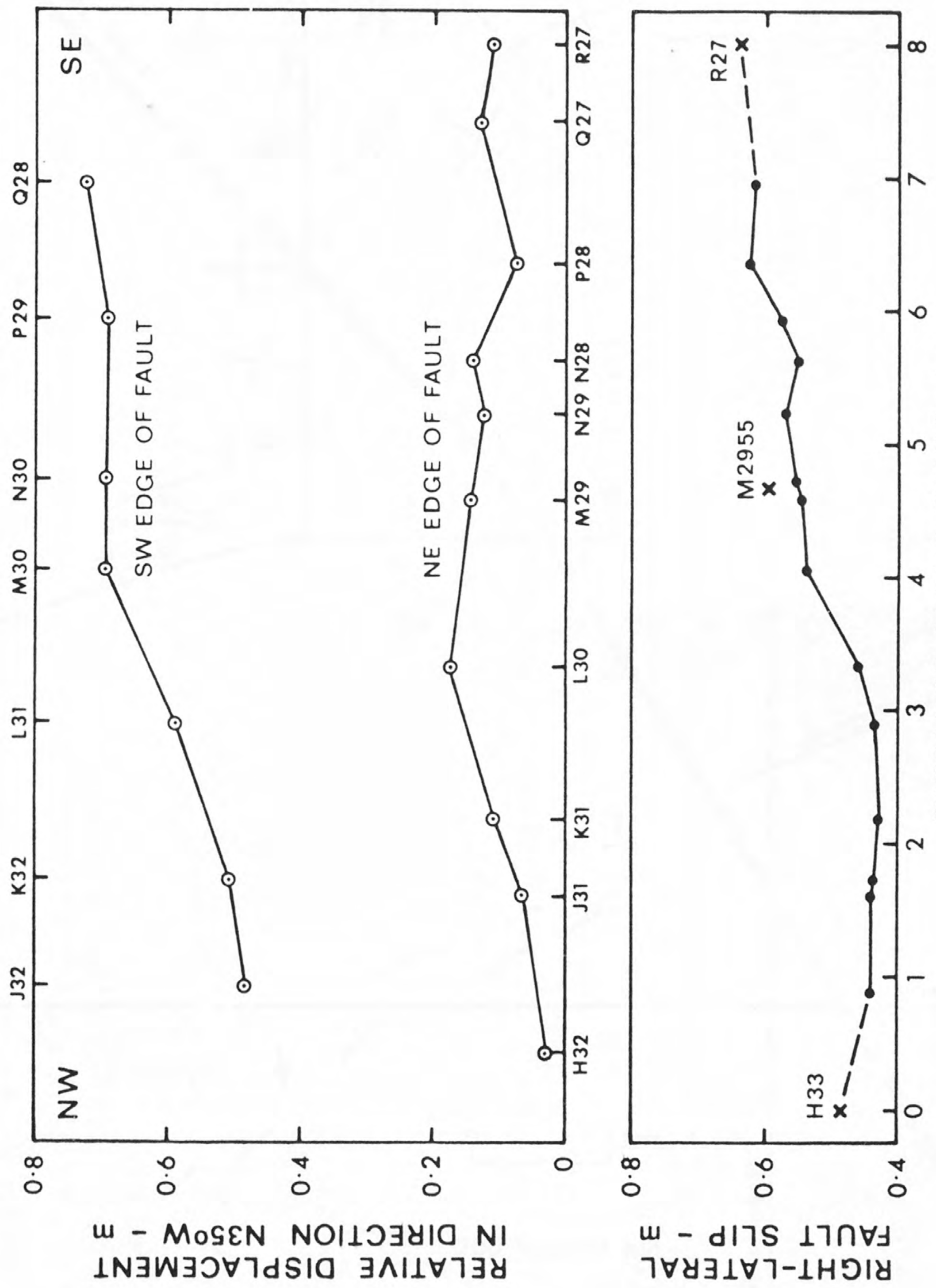

Figure 6. Relative displacements along the Imperial fault, and inferred slip, corrected for shear strain.

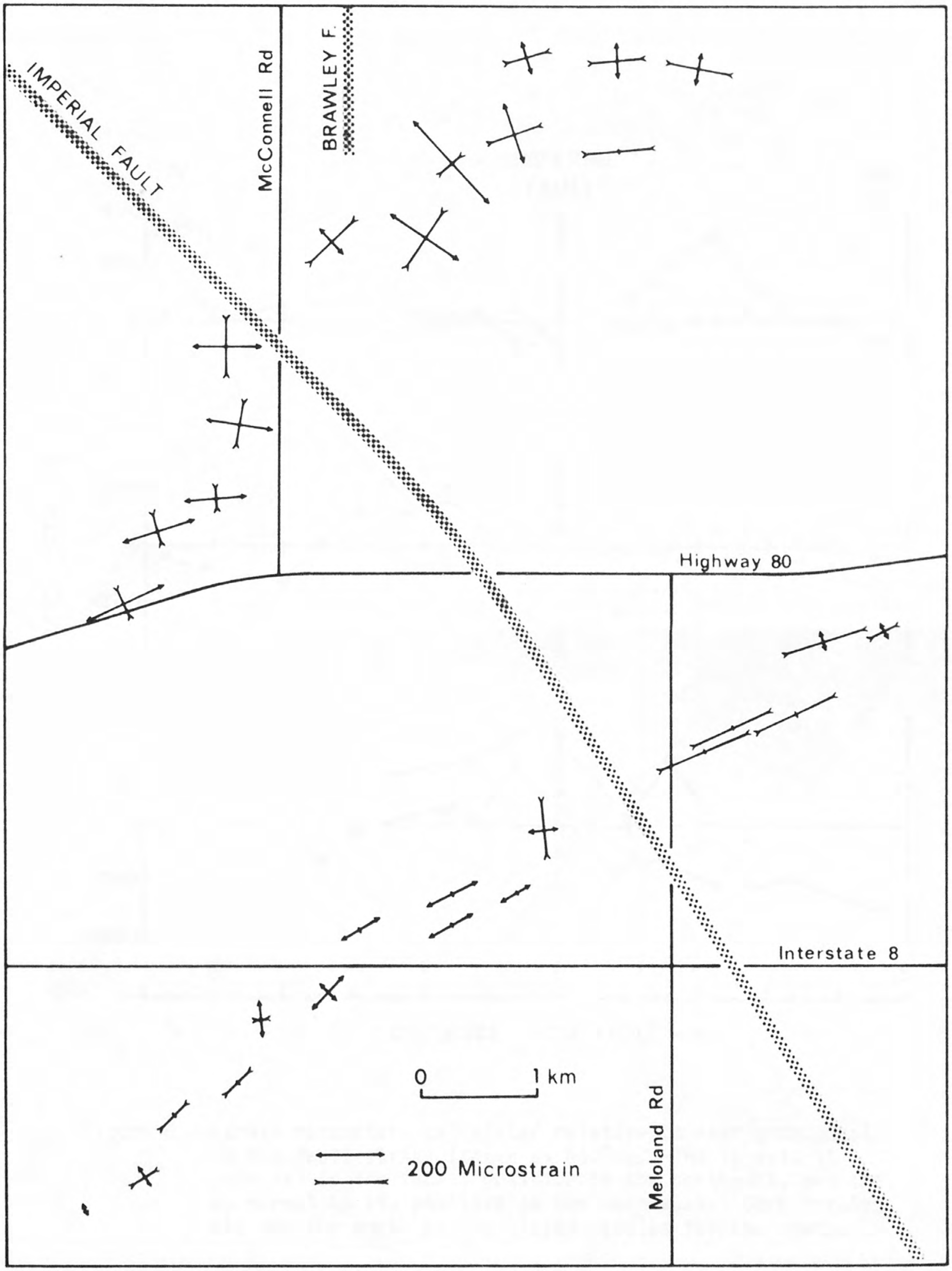

Figure 7. Principal strain axes for the north and south chains. Arrow heads have been omitted for values of less than 25 microstrain.

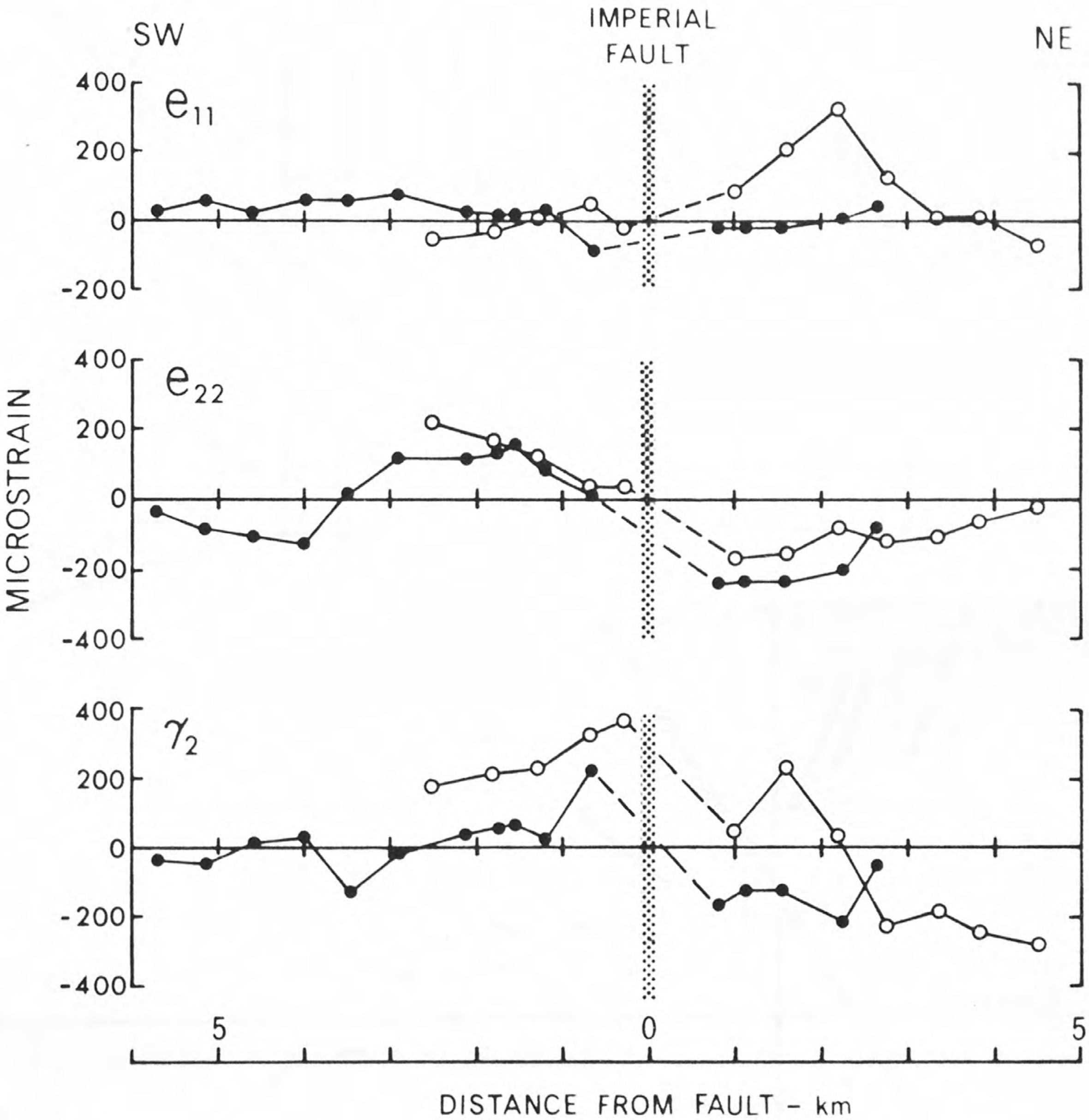

Figure 8. Strain parameters calculated relative to axes orthogonal to the fault strike (taken as N40°W). The x_1 axis is parallel to the fault, positive to the southeast, and the x_2 normal to it, positive to the northeast. Open circles are for the north chain, closed circles for the south.

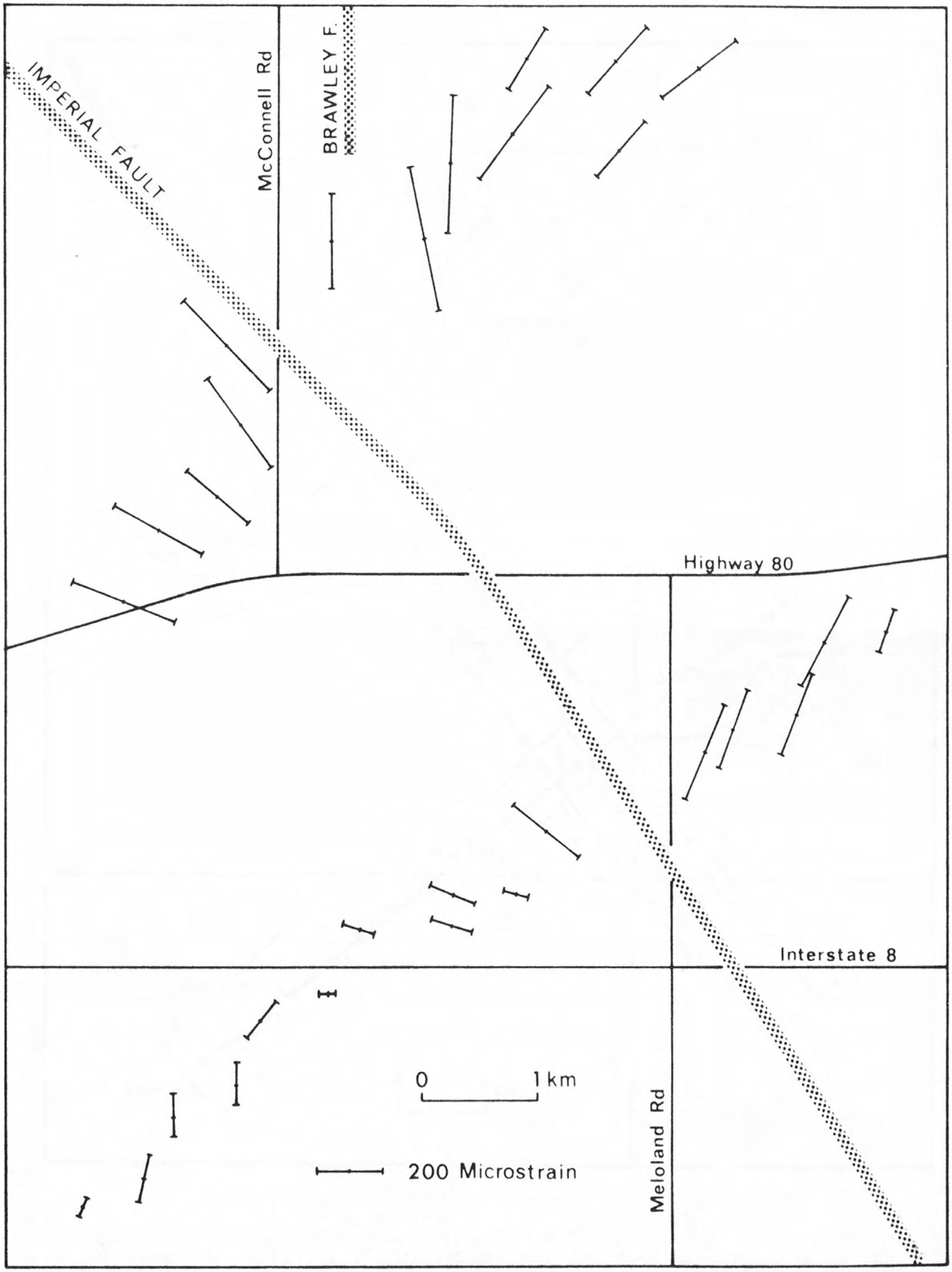

Figure 9. Directions and magnitudes of the maximum right-lateral shear strain for the north and south chains.

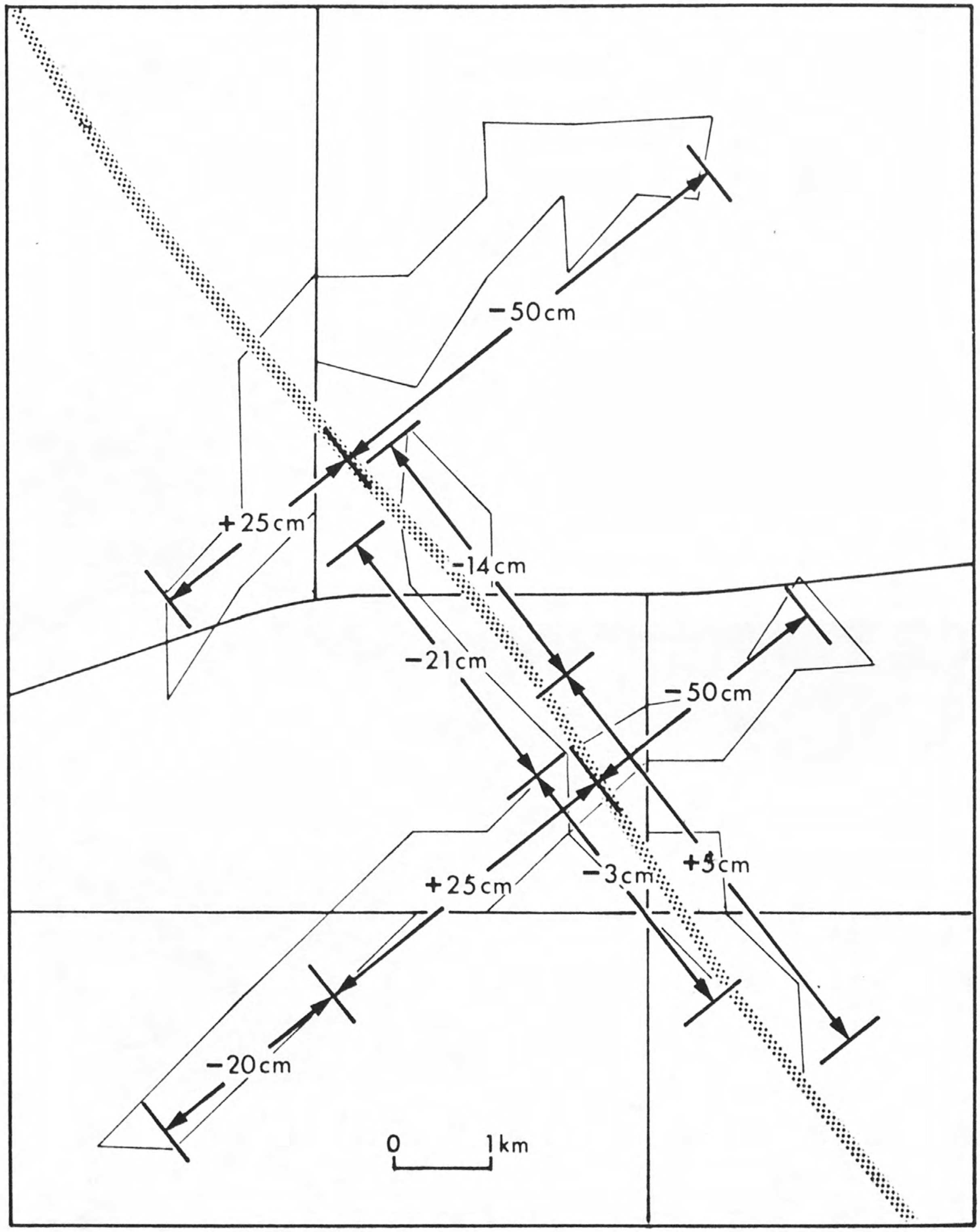

Figure 10. Relative displacements derived from measurements of the north, south and fault chains.